
Figures and figure supplements

PRMT5 regulates ovarian follicle development by facilitating *Wt1* translation

Min Chen *et al*

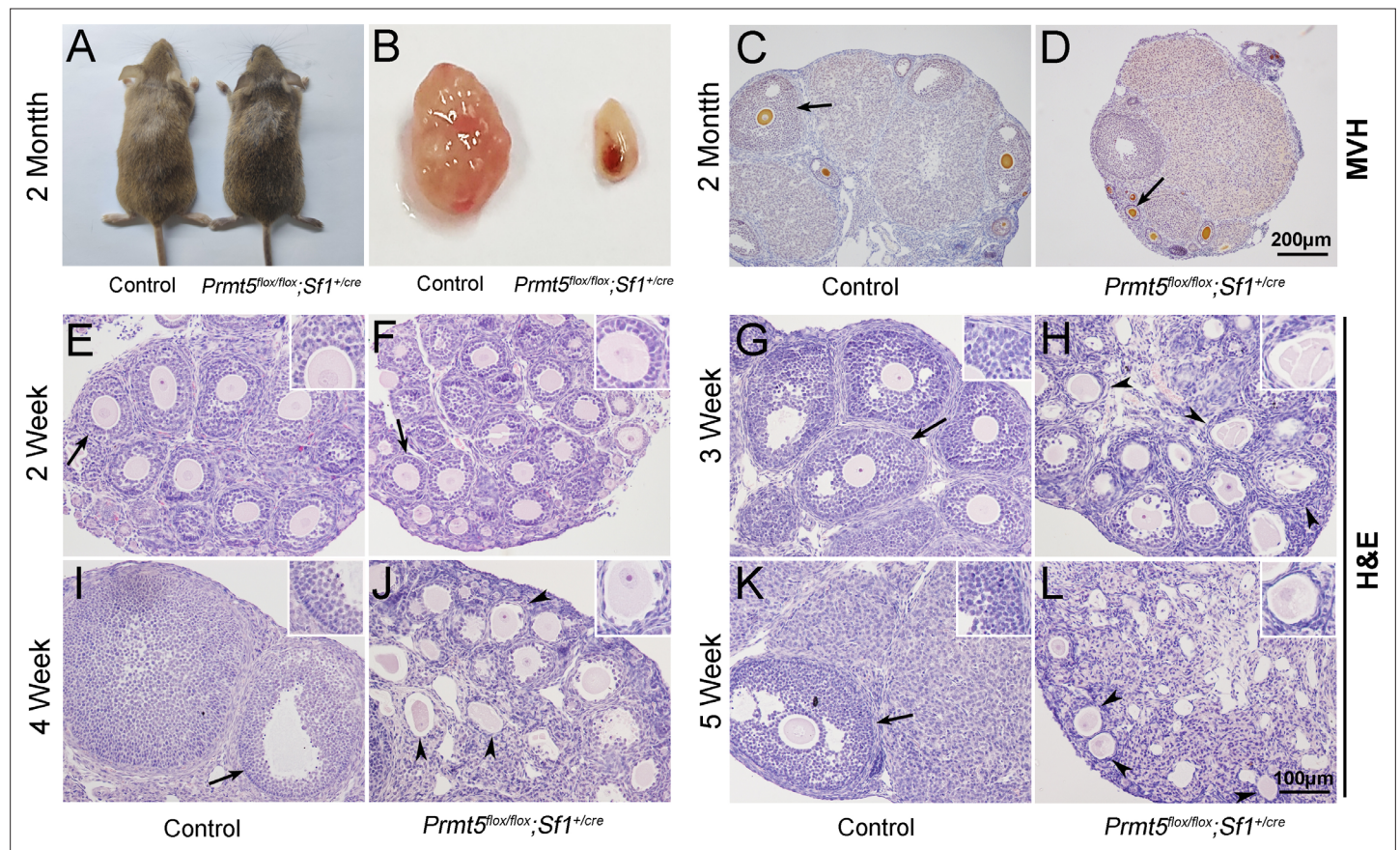


Figure 1. Loss of *Prmt5* in granulosa cells caused aberrant follicle development and female infertility. No developmental abnormalities were observed in *Prmt5^{flox/flox};Sf1^{+/cre}* mice (A) at 2 months of age, and the ovary size was dramatically reduced (B). Histology of ovaries from control (C) and *Prmt5^{flox/flox};Sf1^{+/cre}* mice (D) at 2 months of age. The histology of ovarian follicles was grossly normal in *Prmt5^{flox/flox}* mice at 2 weeks (F, black arrows). Defects in follicle development were observed in *Prmt5*-mutant mice at 3 weeks (H, black arrowheads). Aberrant ovarian follicles with disorganized granulosa cells were observed in *Prmt5^{flox/flox};Sf1^{+/cre}* mice at 4 (J, black arrowheads) and 5 (L, black arrowheads) weeks of age. (E), (G), (I), (K) are the histology of ovarian follicles in control mice respectively at 2, 3, 4, and 5 weeks.

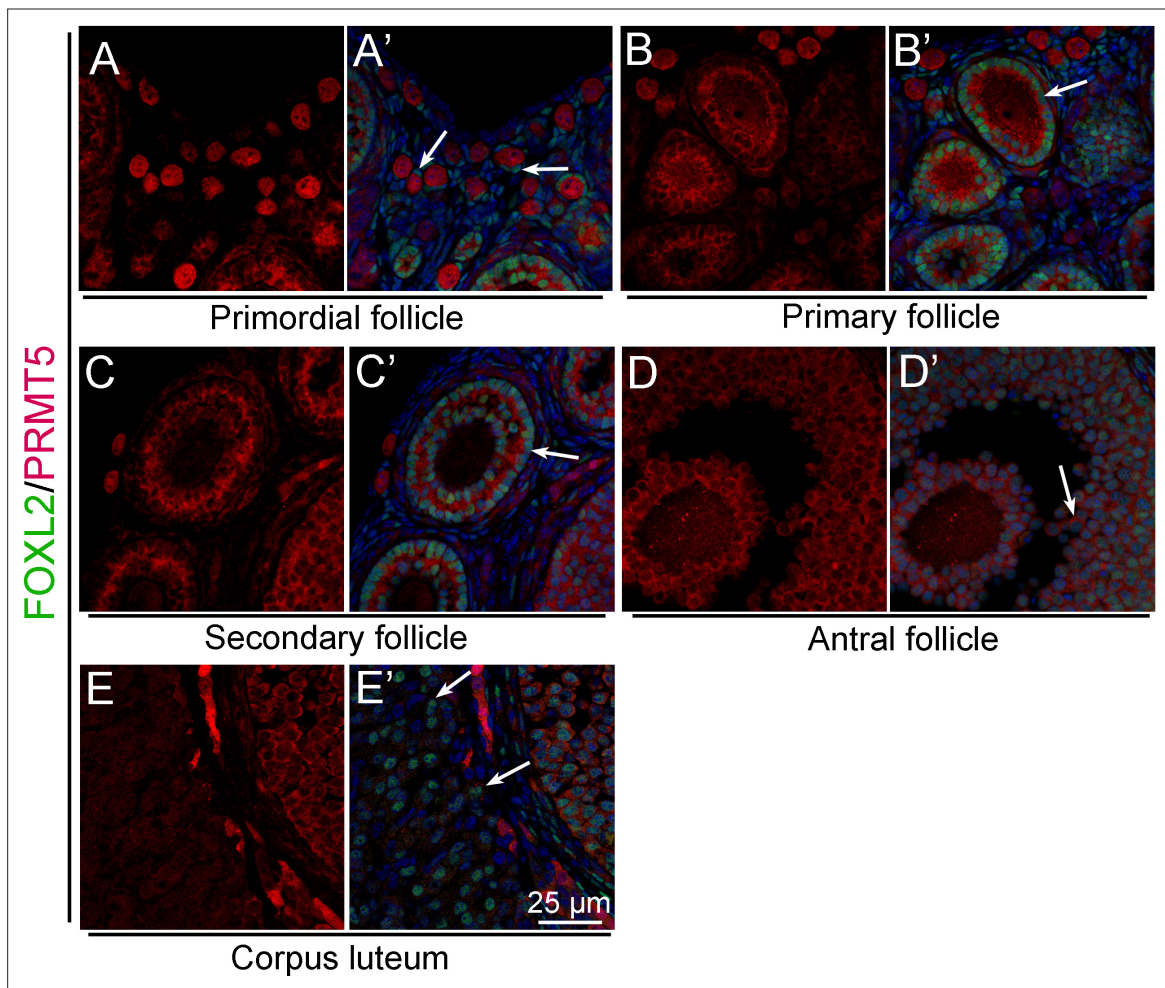


Figure 1—figure supplement 1. PRMT5 was expressed in granulosa cells of growing follicles. The expression of PRMT5 was examined by immunofluorescence (red), and granulosa cells were labeled with FOXL2 (green). PRMT5 was not expressed in granulosa cells of primordial follicles (**A**, **A'**, white arrows). PRMT5 was expressed in granulosa cells of primary follicles (**B**, **B'**, white arrows), secondary follicles (**C**, **C'**, white arrows), and antral follicles (**D**, **D'**, white arrows). No PRMT5 signal was detected in the corpus luteum (**E**, **E'**, white arrows). DAPI (blue) was used to stain the nuclei.

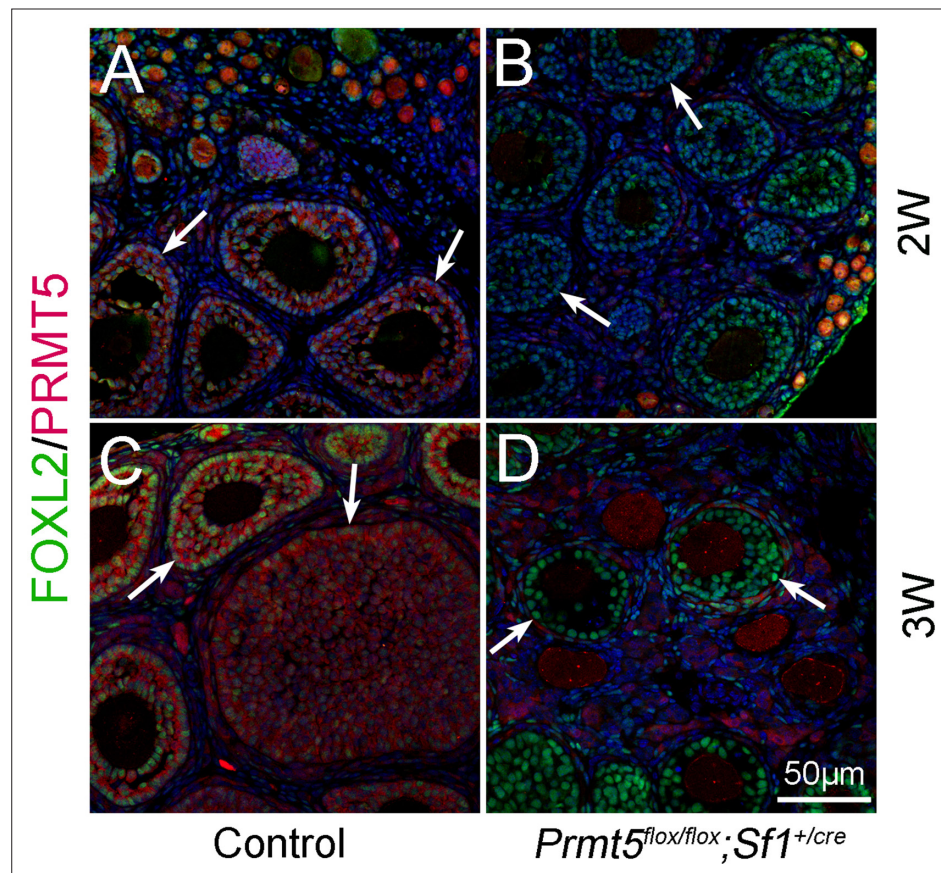


Figure 1—figure supplement 2. *Prmt5* was deleted in granulosa cells of *Prmt5^{flox/flox};Sf1^{+/-cre}* mice. The expression of PRMT5 was examined by immunofluorescence (red), and granulosa cells were labeled with FOXL2 (green). PRMT5 protein was detected in granulosa cells of control ovaries at 2 weeks (**A**, white arrows) and 3 weeks (**C**, white arrows) after birth. No PRMT5 signal was detected in granulosa cells of *Prmt5^{flox/flox};Sf1^{+/-cre}* ovaries at 2 weeks (**B**, white arrows) and 3 weeks (**D**, white arrows). DAPI (blue) was used to stain the nuclei.

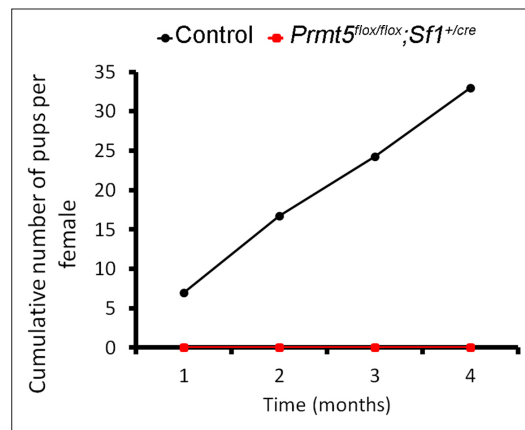


Figure 1—figure supplement 3. Female *Prmt5^{flox/flox}; Sf1^{+/-cre}* mice were infertile. Continuous breeding assay was performed with control and *Prmt5^{flox/flox}; Sf1^{+/-cre}* female mice (n = 4 per genotype) starting at 8 weeks of age. Both control and *Prmt5^{flox/flox}; Sf1^{+/-cre}* female mice were crossed with wild-type male mice. The average cumulative number of pups per female is shown.

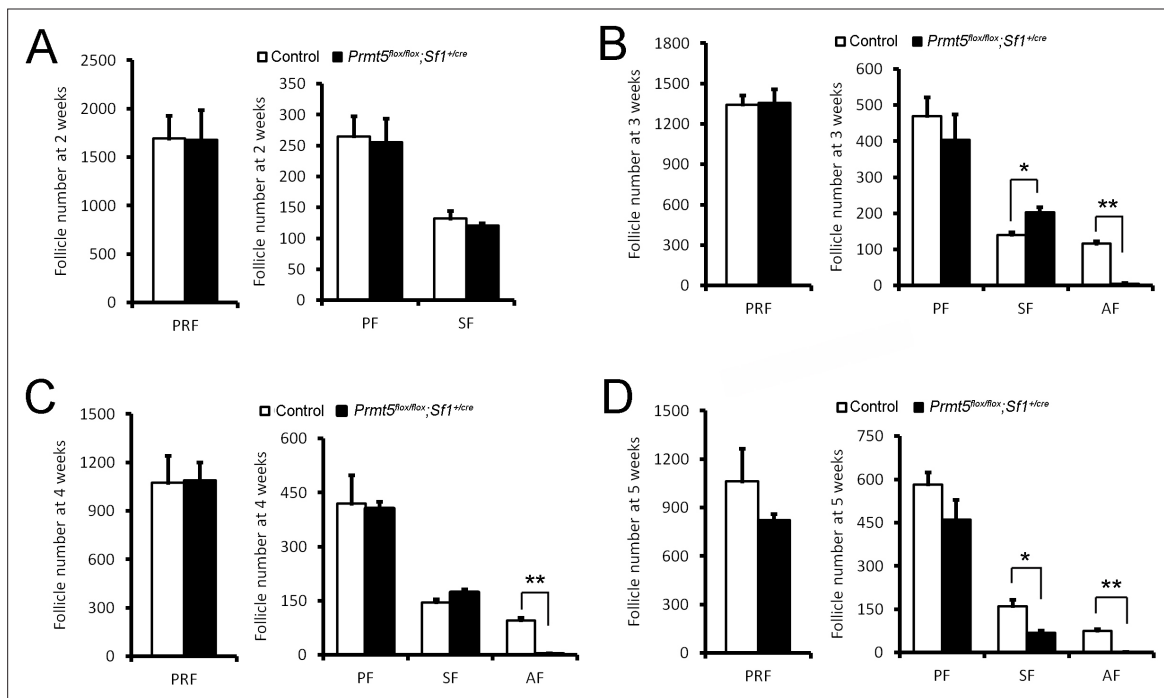


Figure 1—figure supplement 4. Follicle development was arrested at the secondary stage. The number of primordial (PRF), primary (PF), secondary (SF), and antral follicles (AF) was counted and quantified in control and *Prmt5^{flox/flox};Sf1^{+/-cre}* female mice at 2 (A), 3 (B), 4 (C), and 5 (D) weeks of age. Few antral follicles could be observed in ovaries of *Prmt5^{flox/flox};Sf1^{+/-cre}* mice. The data are presented as the mean \pm SEM (n = 3). *p<0.05. **p<0.01.

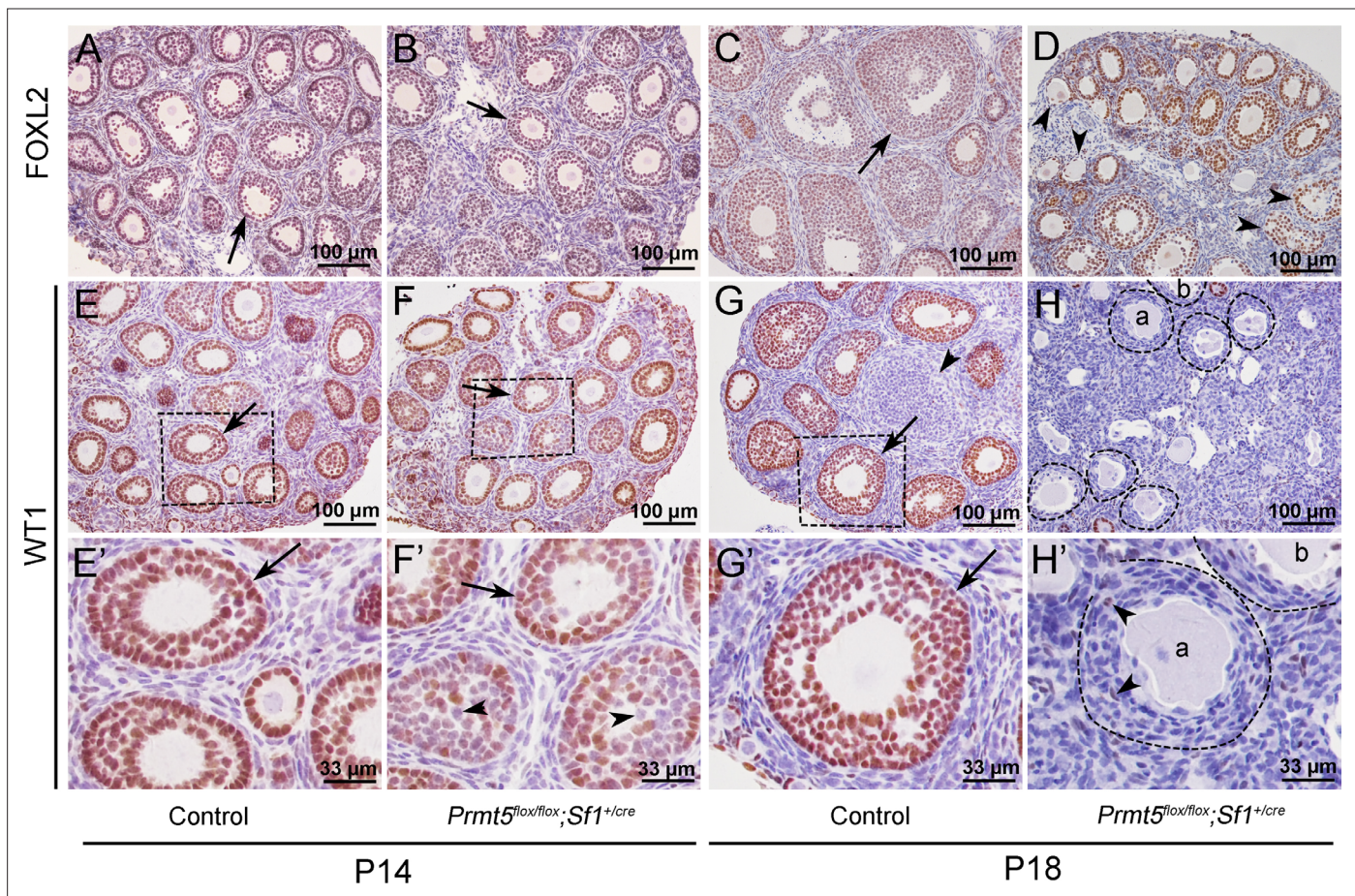


Figure 2. The expression of WT1 was dramatically reduced in the granulosa cells of *Prmt5^{flox/flox}; Sf1^{+/-cre}* mice at P18. The expression of FOXL2 and WT1 in granulosa cells of control and *Prmt5^{flox/flox}; Sf1^{+/-cre}* mice was examined by immunohistochemistry. FOXL2 protein was expressed in the granulosa cells of both control (A, C) and *Prmt5^{flox/flox}; Sf1^{+/-cre}* mice (B, D) at P14 and P18. WT1 protein was expressed in granulosa cells of primordial, primary, and secondary follicles in control mice at P14 and P18 (E, E', G, G', black arrows). WT1 expression was absent from most granulosa cells in *Prmt5^{flox/flox}; Sf1^{+/-cre}* mice at P18 (H, H'); only very few granulosa cells were WT1-positive (H', black arrowheads). (E'–H') are the magnified views of (E–H) respectively.

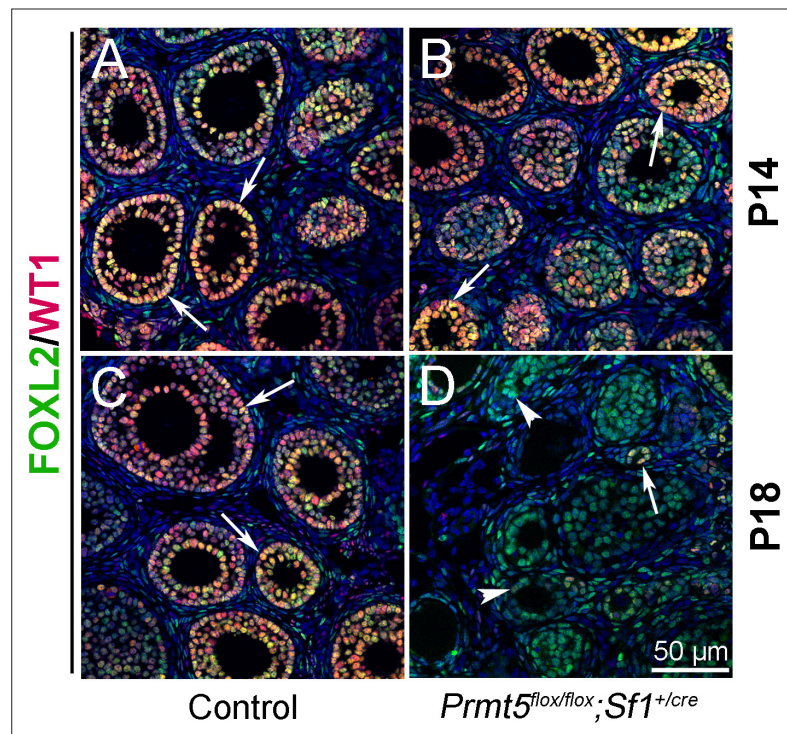


Figure 2—figure supplement 1. WT1 expression was decreased significantly in *Prmt5^{flox/flox}; Sf1^{+/-cre}* granulosa cells at P18. The expression of FOXL2 (green) and WT1 (red) in ovaries of control (A, C) and *Prmt5^{flox/flox}; Sf1^{+/-cre}* (B, D) mice at P14 and P18 was examined by immunofluorescence. WT1 expression was decreased dramatically in *Prmt5^{flox/flox}; Sf1^{+/-cre}* granulosa cells at P18 (D, arrowheads). Few WT1-positive granulosa cells remained (D, arrows). DAPI (blue) was used to stain the nuclei.

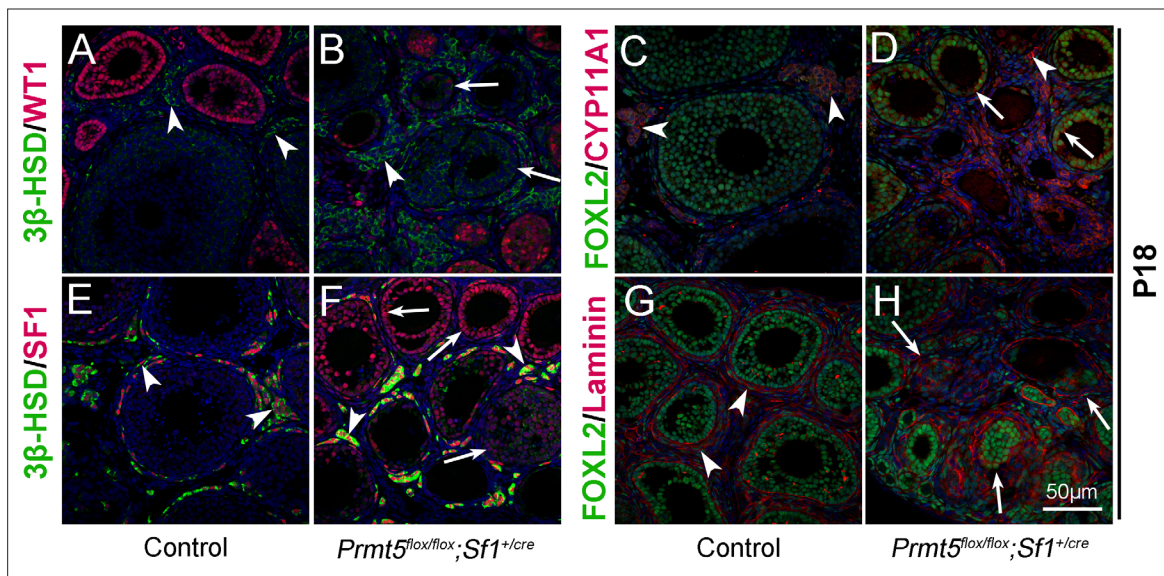


Figure 3. The identity of granulosa cells in *Prmt5^{lox/lox};Sf1^{+/-cre}* mice was changed. The expression of 3 β -HSD, WT1, FOXL2, CYP11A1, and SF1 in ovaries of control and *Prmt5^{lox/lox};Sf1^{+/-cre}* mice at P18 was examined by immunofluorescence. In control ovaries, 3 β -HSD (A), CYP11A1 (C), and SF1 (E) were expressed only in theca-interstitial cells (white arrowheads). In the ovaries of *Prmt5^{lox/lox};Sf1^{+/-cre}* mice, 3 β -HSD (B), CYP11A1 (D), and SF1 (F) were also detected in granulosa cells (white arrows). Compared to the intact follicle structure in control ovaries (arrowheads, G), the follicle structure was disordered in *Prmt5^{lox/lox};Sf1^{+/-cre}* ovaries (arrows, H) as shown by Laminin expression. DAPI (blue) was used to stain the nuclei.

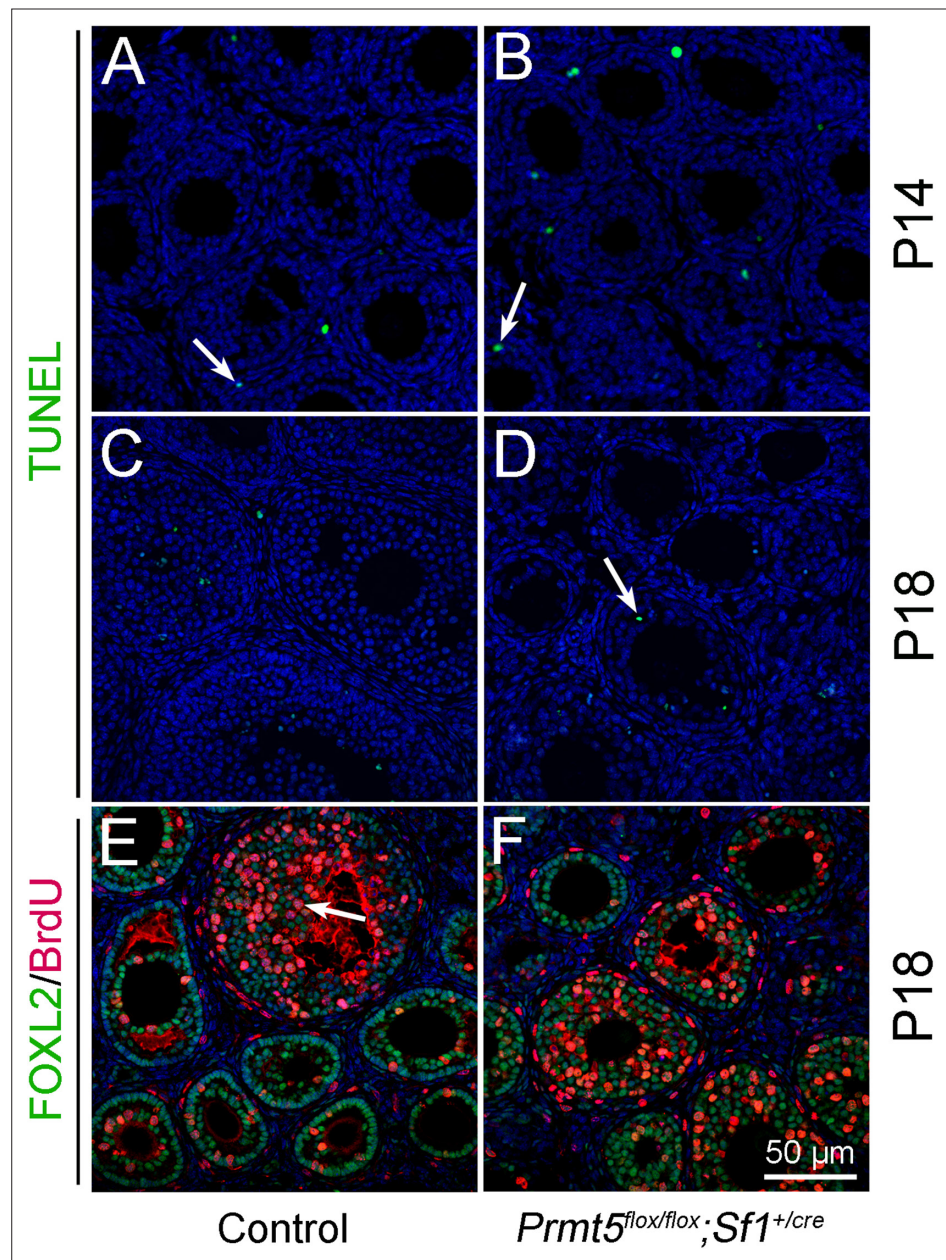


Figure 3—figure supplement 1. The apoptosis and proliferation of granulosa cells were not changed in *Prmt5^{flox/flox};Sf1^{+/-cre}* mice at P14 and P18. Apoptosis and cell proliferation were assessed by TUNEL assay (A–D) and BrdU incorporation assay (E, F), respectively. The numbers of TUNEL-positive cells and BrdU-positive cells were not different in *Prmt5^{flox/flox};Sf1^{+/-cre}* ovaries compared to control ovaries. DAPI (blue) was used to stain the nuclei.

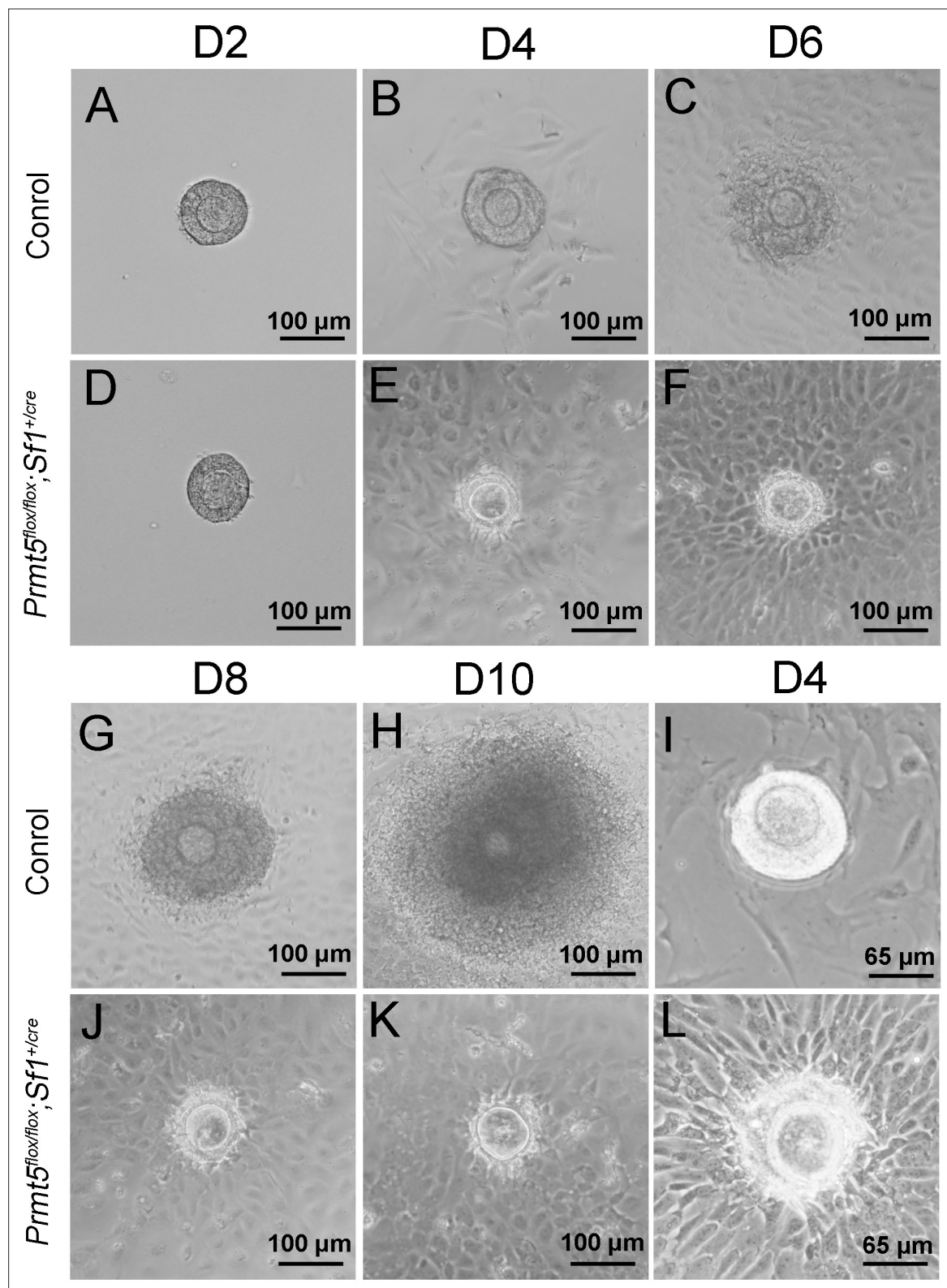


Figure 3—figure supplement 2. Aberrant development of in vitro-cultured *Prmt5^{flox/flox}; Sf1^{+/-cre}* follicles. Follicles with 2–3 layers of granulosa cells isolated from control and *Prmt5^{flox/flox}; Sf1^{+/-cre}* mice were cultured in vitro. After 9 days of culture, control follicles grew significantly and developed to the preovulatory stage (A–C, G, H). No obvious layers of granulosa cells were observed around oocytes (D–F, J, K), and the granulosa cells extended away from the oocytes and adhered to the dish (L). (I) and (L) are two magnified views of cultured follicles at day 4.

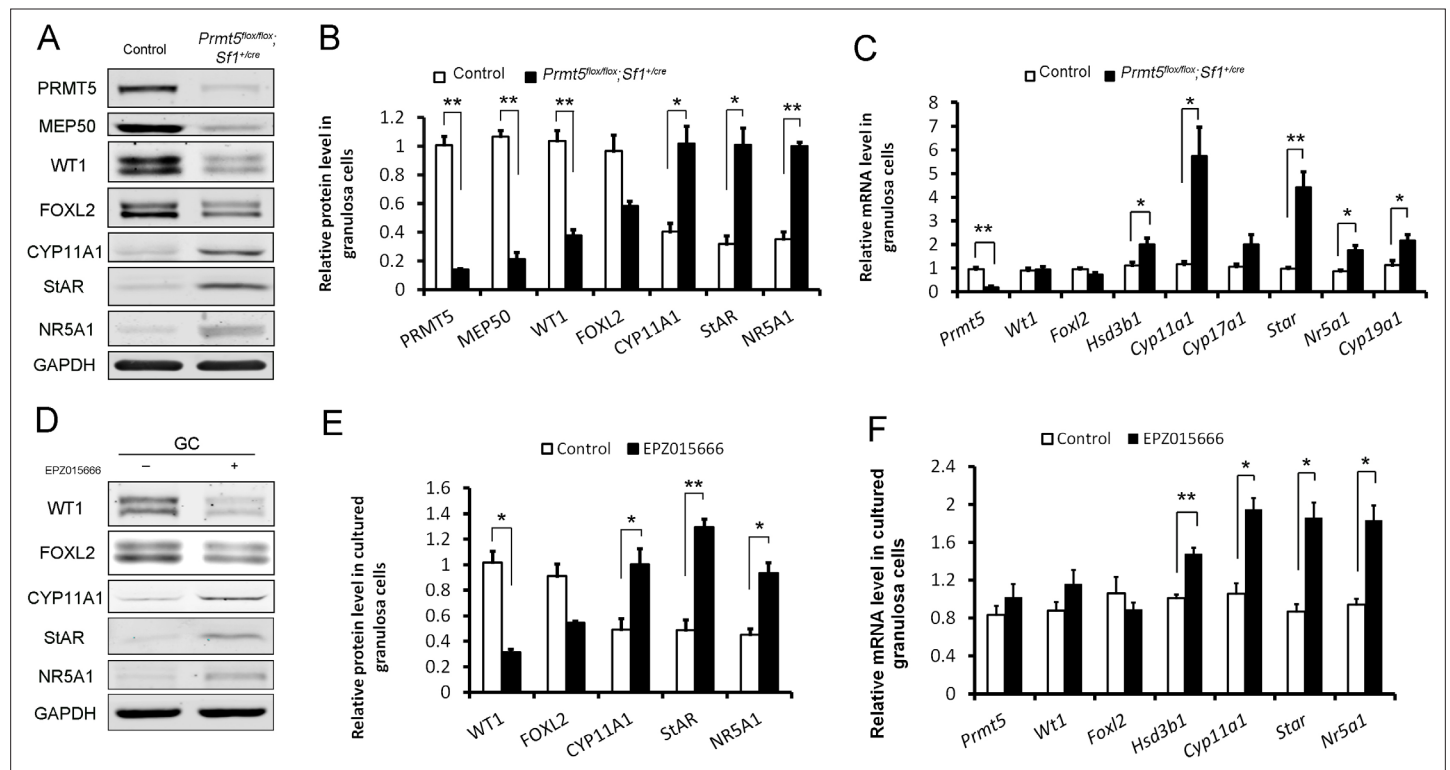


Figure 4. Differentially expressed genes in *Prmt5*-deficient granulosa cells. Western blot (**A**, **D**) and real-time PCR analyses (**C**) of the indicated genes in granulosa cells isolated from control or *Prmt5^{lox/lox}; Sf1^{+/-cre}* ovaries at P18. Western blot (**D**, **E**) and real-time PCR analyses (**F**) of the indicated genes in granulosa cells treated with DMSO or EPZ015666 (5 μ M) for 5 days. The protein expression of three independent experiments in western blot analysis was quantified and normalized to that of GAPDH (**B**, **E**). The data are presented as the mean \pm SEM. For (**B**, **E**, **F**), $n = 3$; for (**C**), $n = 5$. * $p < 0.05$. ** $p < 0.01$.

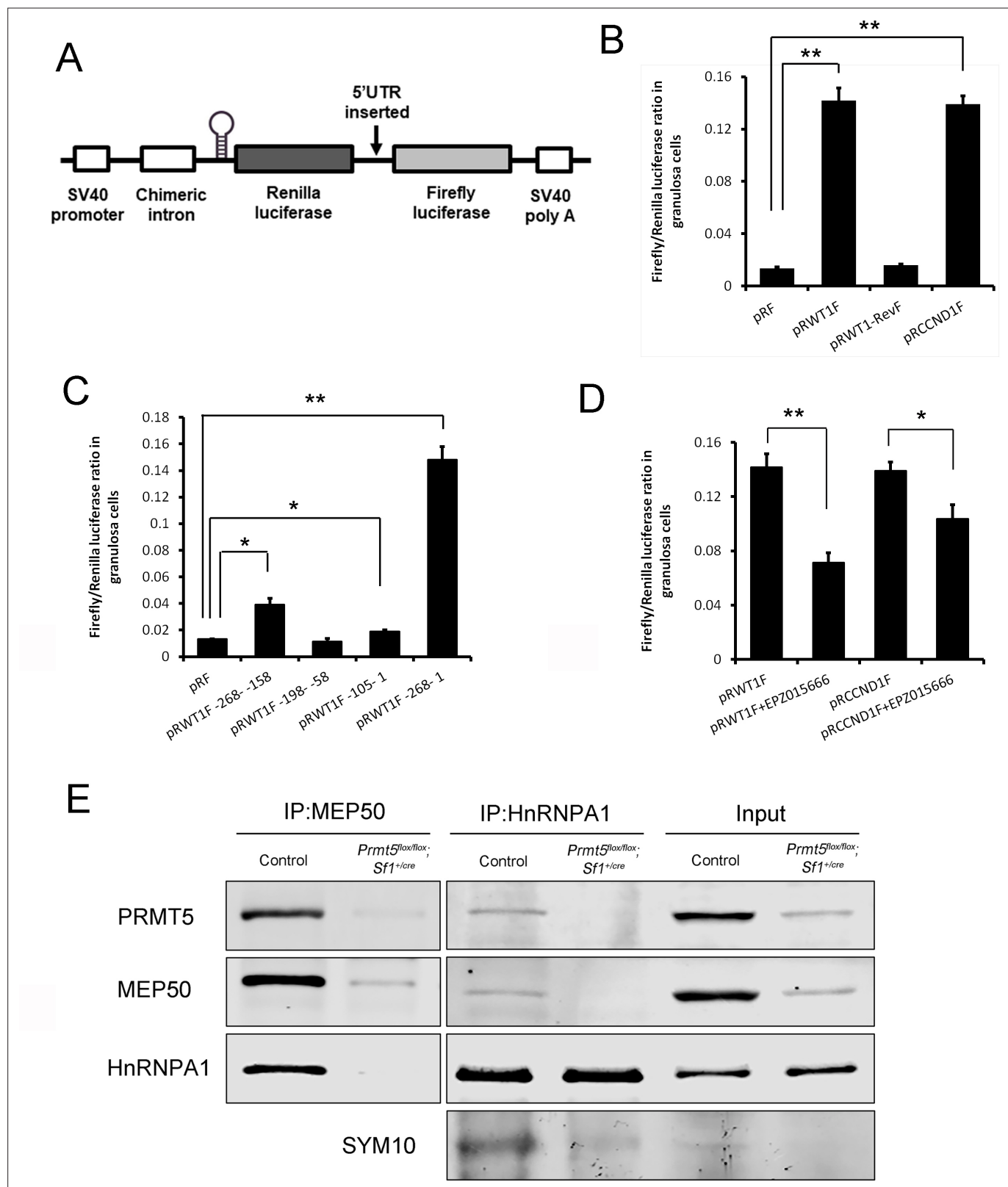


Figure 5. PRMT5 regulated translation of *Wt1* mRNA by inducing internal ribosome entry site (IRES) activity in the 5'UTR. **(A)** Schematic representation of the dicistronic reporter construct. **(B)** *Wt1* 5'UTR has IRES activity. Cultured primary granulosa cells were transfected with pRF, pRWT1F (pRF with the *Wt1* 5'UTR inserted), pRWT1-RevF (pRF with the *Wt1* 5'UTR inserted in reverse orientation), or pRCCND1F (pRF with the *Ccnd1* 5'UTR inserted). The Firefly and Renilla luciferase activities were measured 24 hr later, and the ratios of Firefly luciferase activity to Renilla luciferase activity were calculated.

Figure 5 continued on next page

Figure 5 continued

(C) The full length of *Wt1* 5'UTR is required for maximal luciferase activity. Three fragments of *Wt1* 5'UTR were inserted into pRF construct (pRWT1F –268 to –158, pRWT1F –198 to –58, pRWT1F –105 to –1) and the constructs were transfected into primary granulosa cells. 24 hr later, the cells were harvested for luciferase activity analysis. (D) Luciferase activity was decreased in primary granulosa cells treated with the PRMT5 inhibitor EPZ015666. Isolated granulosa cells were treated with DMSO or EPZ015666 for 4 days. The day granulosa cells were isolated was denoted as day 1. On day 4, granulosa cells were transfected with pRWT1F or pRCCND1F. 24 hr later, the cells were harvested for luciferase activity analysis. The ratios of Firefly luciferase activity to Renilla luciferase activity were calculated. In (B–D), the data are presented as the mean \pm SEM, $n = 4$. * $p < 0.05$. ** $p < 0.01$. (E) Coimmunoprecipitation experiments were conducted in control and *Prmt5^{fllox/fllox}; Sf1^{+/-cre}* granulosa cells. In control granulosa cells, HnRNPA1 was pulled down with an antibody against the PRMT5-associated protein MEP50; PRMT5 and MEP50 were pulled down by an HnRNPA1 antibody. The symmetric dimethylation of HnRNPA1 was significantly decreased in *Prmt5^{fllox/fllox}; Sf1^{+/-cre}* granulosa cells. Blots are representative of three independent experiments.

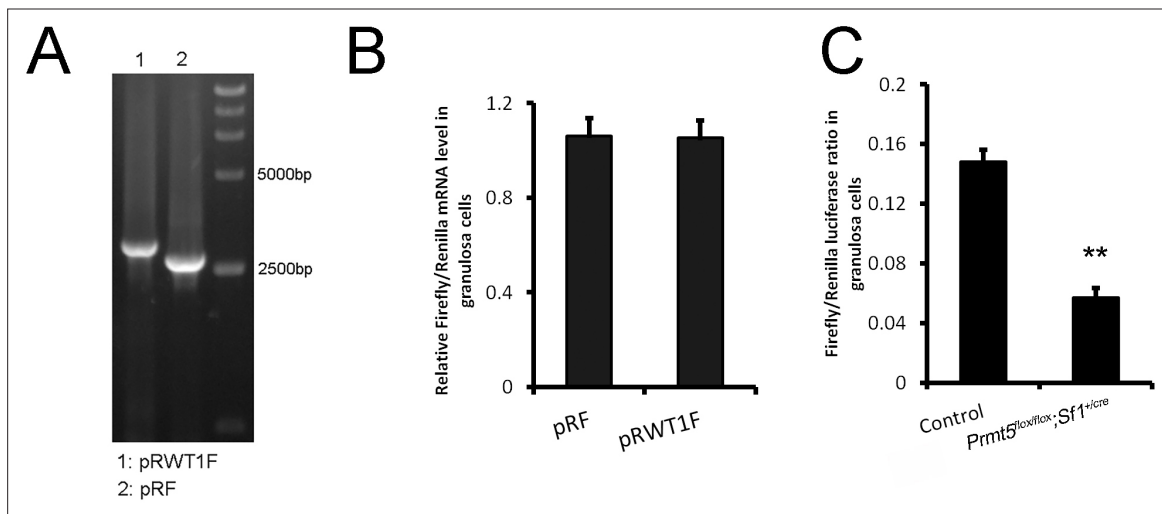


Figure 5—figure supplement 1. The increased luciferase activity of pRWT1F was not due to a monocistronic Firefly open reading frame generated by cryptic splicing or promoter within the dicistronic gene. **(A)** Primary granulosa cells were transfected with pRF or pRWT1F plasmids. RNA was isolated, DNase-treated, reverse-transcribed, and amplified using PCR primers that bind to the 5' end of Renilla luciferase and the 3' end of the Firefly luciferase sequence **(A)** or processed for real-time PCR assays to analyze Firefly and Renilla luciferase mRNA levels **(B)**. The expression of Firefly luciferase mRNA was normalized to that of Renilla luciferase mRNA. **(C)** *Wt1* internal ribosome entry site (IRES) activity was significantly decreased in *Prmt5*-deficient granulosa cells. Control and *Prmt5^{flox/flox}; Sf1^{+/cre}* granulosa cells were transfected with pRWT1F plasmids. 24 hr later, the cells were harvested for luciferase activity analysis. In **(B)** ($n = 3$) and **(C)** ($n = 4$), the data are presented as the mean \pm SEM. ** $p < 0.01$.

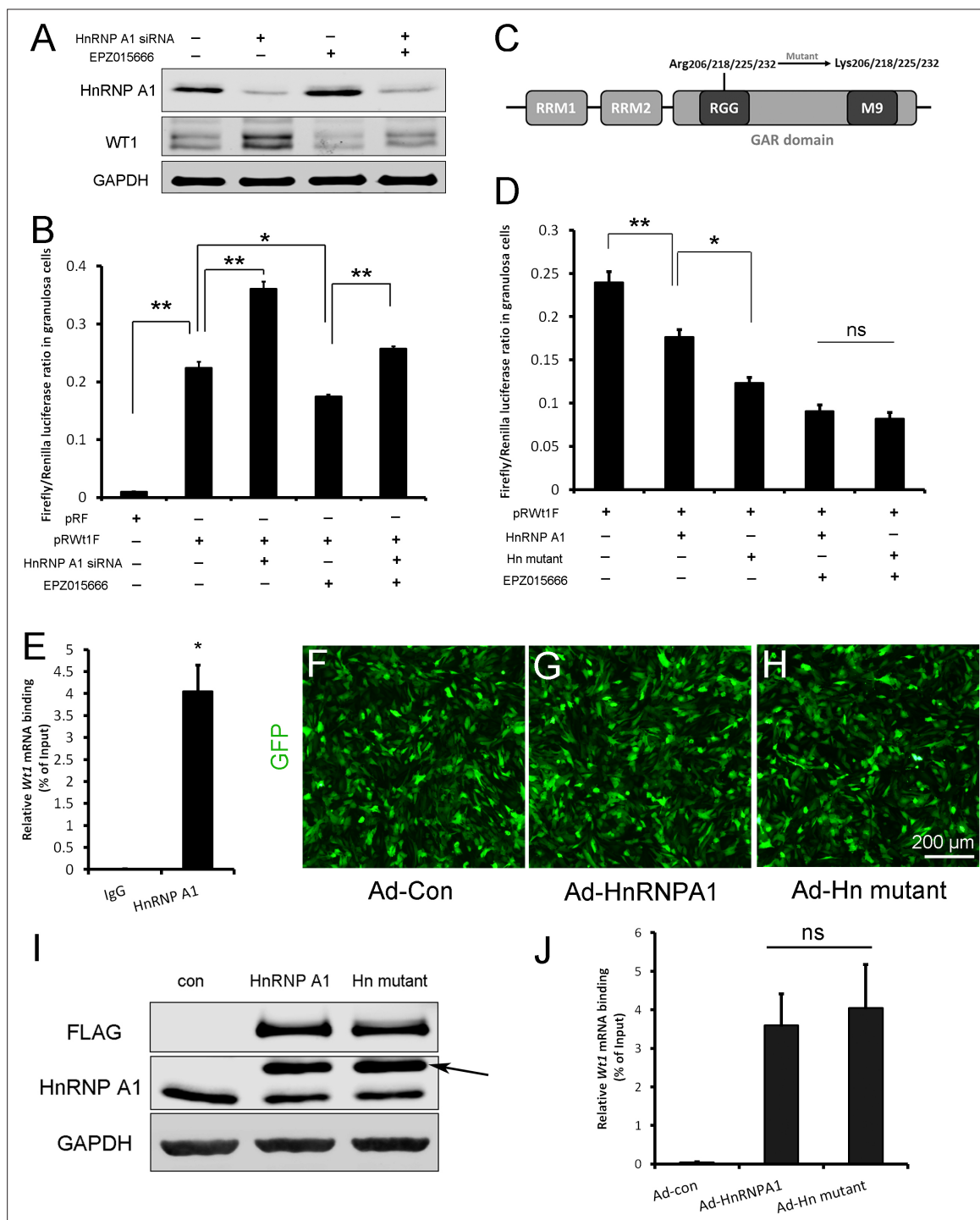


Figure 6. Wt1 internal ribosome entry site (IRES) activity is regulated by PRMT5 via methylation of HnRNP A1. **(A)** Western blot analysis of HnRNP A1 and WT1 in granulosa cells after HnRNP A1 siRNA transfection or EPZ015666 treatment. **(B)** Luciferase activity analysis of pRWT1F in granulosa cells after HnRNP A1 siRNA transfection or EPZ015666 treatment. Isolated granulosa cells were treated with DMSO or EPZ015666 for 4 days. The day granulosa cells isolated is denoted as day 1. On day 2, cells were transfected with control siRNA or siRNA to HnRNP A1. 48 hr later, pRF or pRWT1F were transfected. The luciferase activity of pRWT1F was calculated as the ratio of Firefly luciferase activity to Renilla luciferase activity. **(C)** Schematic diagram of HnRNP A1 protein domains. HnRNP A1 contains two RNA recognition motifs (RRMs). The glycine/arginine-rich (GAR) domain contains an RGG (Arg-Gly-Gly) box and a nuclear targeting sequence (M9). Four arginine residues within the RGG motif were mutated to lysine. **(D)** Luciferase activity analysis of pRWT1F in granulosa cells after EPZ015666 treatment or overexpressing HnRNP A1 or arginine-mutated HnRNP A1. Isolated granulosa cells were treated with DMSO or EPZ015666 for 4 days. On day 3, flag-tagged HnRNP A1 or mutant plasmids were cotransfected with pRWT1F into granulosa cells. 48 hr later, cells were harvested for luciferase activity analysis. **(E)** RNA immunoprecipitation was conducted in granulosa cells using an HnRNP A1

Figure 6 continued on next page

Figure 6 continued

antibody, and the *Wt1* mRNA pulled down by HnRNPA1 was analyzed with real-time PCR. **(F–H)** Primary granulosa cells were cultured and infected with control, flag-tagged HnRNPA1, or mutant HnRNPA1 (Ad-Hn mutant) adenoviruses. The expression of control and mutant HnRNPA1 was examined by western blot analysis **(I)**. **(J)** RNA immunoprecipitation was conducted using a FLAG antibody, and *Wt1* mRNA pulled down by control or mutant HnRNPA1 protein was analyzed with real-time PCR. For **(B, D)** ($n = 4$) and **(E, J)** ($n = 3$), the data are presented as the mean \pm SEM. * $p < 0.05$. ** $p < 0.01$.

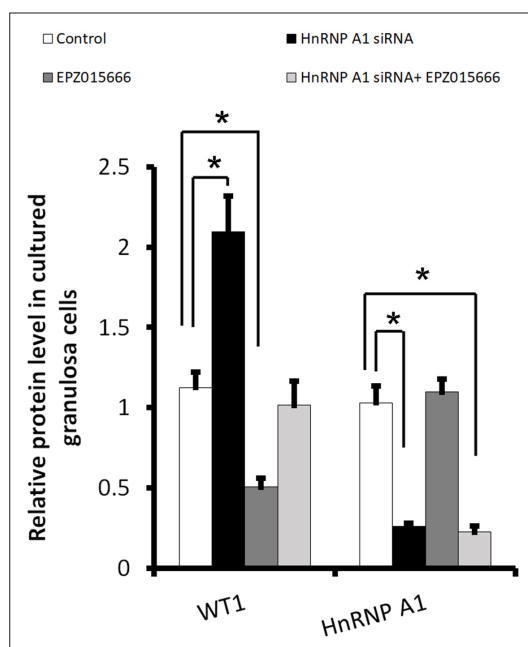


Figure 6—figure supplement 1. Quantitative analysis of HnRNP A1 and WT1 protein expression in granulosa cells after HnRNP A1 siRNA transfection or EPZ015666 treatment. The protein expression of HnRNP A1 and WT1 in **Figure 6A** was quantified of three independent experiments and normalized to that of GAPDH. The data are presented as the mean \pm SEM (n = 3). *p<0.05.

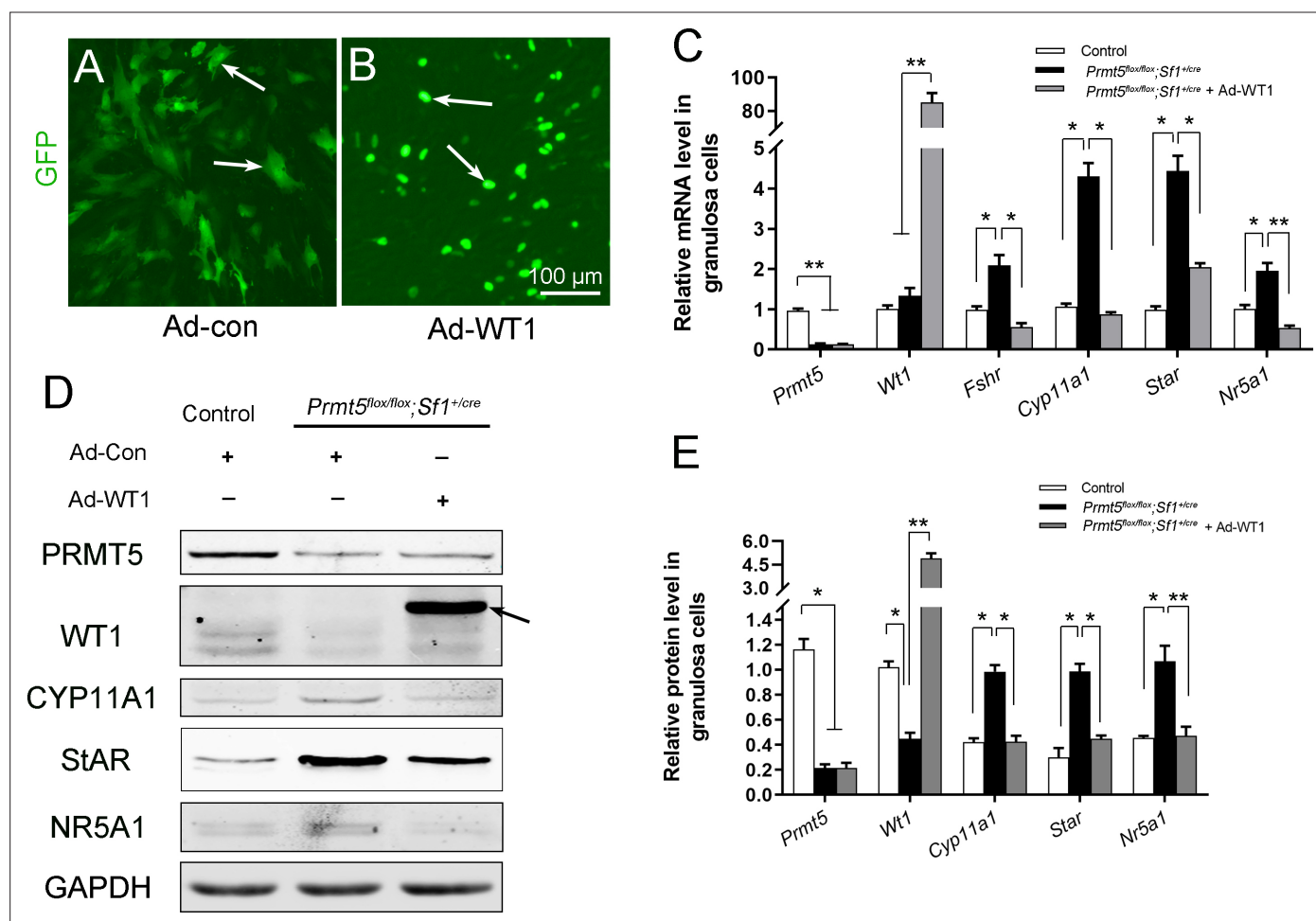


Figure 7. The upregulation of steroidogenic genes in $Prmt5^{flox/flox}; Sf1^{+/-cre}$ granulosa cells was reversed by $Wt1$ overexpression. **(A, B)** Granulosa cells isolated from control and $Prmt5^{flox/flox}; Sf1^{+/-cre}$ mice were cultured and infected with control or GFP-fused $Wt1$ adenovirus. The expression of steroidogenic genes was examined by RT-qPCR **(C)** and western blot analysis **(D)**. The protein expression of three independent experiments in western blot analysis was quantified and normalized to that of GAPDH **(E)**. **(C, E)** The data are presented as the mean \pm SEM ($n = 3$). * $p < 0.05$. ** $p < 0.01$.

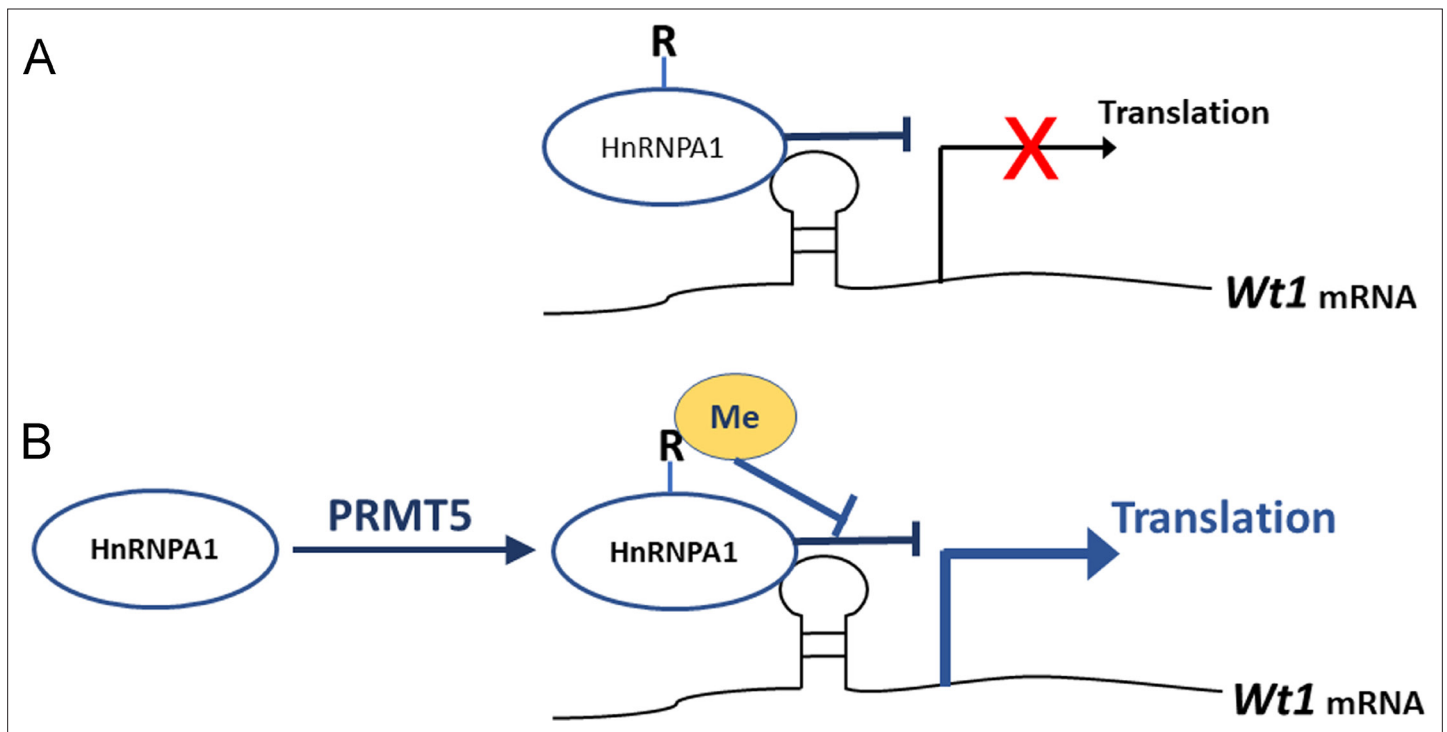


Figure 8. Schematic illustration of how PRMT5 regulates *Wt1* mRNA translation. **(A)** As an ITAF, HnRNPA1 binds to *Wt1* mRNA and inhibits the internal ribosome entry site (IRES)-dependent translation of *Wt1*. **(B)** PRMT5 catalyzes symmetric methylation of HnRNPA1, which suppresses the ITAF activity of HnRNPA1 and promotes the translation of *Wt1* mRNA. R: arginine. Me: methylation.